Corpus Callosum Shape Changes in Early Alzheimer's Disease: An MRI Study Using the Automatic Deformable Model

Amira Ben Rabeh, Faouzi Benzarti, Hamid Amiri
Signal, image and technology information (LR-SITI)
National Engineering School of Tunis (ENIT), Manar, Tunisia
Emails: amira.benrabeh@gmail.com benzartif@yahoo.fr hamidlamiri@yahoo.fr

Mouna Bouaziz
Radiology Service, Institut MT Kassab
Hospital Kassab, Ksar Said, Tunis,Tunisia
Email: bouaziz_mouna@yahoo.fr

***Abstract*—In this paper, we propose a solution to diagnose Alzheimer's pathology; we are interested in changing the shape of the Corpus Callosum (CC). It is the commissure of the brain and Alzheimer diseases manifests by a significant reduction of its volume. To do this, we used a classification method based on decision trees and the Active Shape Model (ASM) to extract the lesion study. For the deformable model, we added the following contribution: integration of a priori knowledge to automate the initialization of the average shape. For the pretreatment step, we used the median filter. Our method is validated by a physician to diagnose Alzheimer's disease.**

***Keywords*—Alzheimer; Corpus Callosum (CC); active shape model (ASM).**

I. INTRODUCTION

Medical images are now ubiquitous in the clinical portion in brain imaging: anatomic imaging (Computed Tomography (CT), Magnetic Resonance Imaging (MRI)), vascular (Magnetic Resonance Angiography (MRA)) and functional (Positron Emission Tomography (PET), Single Photon Emission Computed Tomography (SPECT), Functional Magnetic Resonance Imaging (fMRI), electroencephalography (EEG), magnetoencephalography (MEG)). The amount of information increases even more when multiple images are acquired on the same patient to exploit the complementarity of different ways, or to follow a temporal evolution. Finally, these images are often accompanied by metadata on the patient's history and cerebral pathology. With all these images and complexity, the doctor can usually visually extract it as incomplete information [1]-[4].

In this work, we are particularly interested in the description of the surfaces of the Corpus Callosum and their classification to facilitate the diagnosis of Alzheimer's disease. The shape analysis and classification are part of an indivisible digital compact processing chain and automatic (or semiautomatic) Computer-Aided Diagnosis (CAD). Thus, a good evaluation of the performance of such part of description or classification requires the mastery of the entire chain of diagnosis.

Our work is organized as follows: first, we describe the previous works. In the second section, we define the Corpus Callosum. In the third section, we present our proposed method. In the fourth section, we provide results and discussion.

II. PREVIOUS WORK

There are many methods for diagnosing Alzheimer's diseases, such as:

A. VBM (Voxel Based Morphometry)

VBM is a method developed by Ashburner et al. [5] in 2000. The objective of VBM is to detect significant differences in gray matter between two groups of subjects by voxel to voxel tests. VBM comprises four steps: normalization stereotactic images on the same area, followed by segmentation of the images, and then smoothing the maps of gray matter obtained, and finally, the application of parametric statistical tests voxel to voxel.
It is a performant method but it used just the sagittal section.

B. Method Proposed by Olfa Ben Ahmed

She used the Region of Interest (ROI) to extract the hippocampus and cingulate cortex. For the classification step, it uses the Bag of Visual World (BOVW) method. This approach is applied separately on both ROI (hippocampus and cingulate cortex). The role of this model is to combine the extracted features of each ROI to build a visual vocabulary. In addition, the region differs from one projection to another [6]. Thus, we choose to perform the procedure grouping three times from different projections (sagittal, axial and coronal) and generating a visual vocabulary by projection.

C. ASM+D(Active Shape Method + Distance)

In addition to the a priori knowledge about the shape and deformation modes of the structures studied, this method consists in another acquaintance on the change in the distance between these structures. This new knowledge is estimated in a learning phase which is to be deducted from a set of sample images and based on principal component analysis, a model describing a distance variation space allowed distance between structures [7]. This controls the evolution of initial estimates during the localization phase and ensures the maintenance of the inter-pattern distance in the space allowed.

 ISBN: 978-1-61208-390-2

III. CORPUS CALLOSUM AND ALZHEIMER DISEASE

The Corpus Callosum is a commissure (through union between two parties) section of the brain. The axons beam interconnects the two cerebral hemispheres. This is the largest commissure of the brain because it connects the four lobes of the brain between them (frontal lobes, temporal, parietal and occipital left and right). The Corpus Callosum, therefore, ensures the transfer of information between the two hemispheres and coordination [8]-[13]. Other commissures are the fornix, the anterior cingulate and the commissure. The CC has been a region examined extensively for indications of Alzheimer various pathology [14]-[19]. This manifests by a significant reduction of its volume.

IV. MATERIAL

Our approach is applied to reference MRI based BRAINWEB. The images are a grayscale and size of 500 * 500 pixels. These images are made by experts.

V. PROPOSED METHOD

Our system is presented in Figure 1.

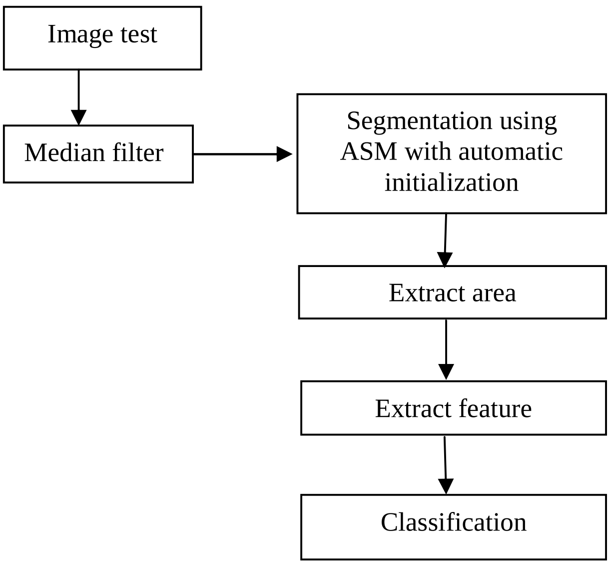

Figure.1. Diagram of the proposed method

A. Median Filter

It is specifically effective against noise pepper and salt in images to grayscale. The operation is to replace the value of a pixel with the median value of all the pixels in its neighborhood.

B. The Active Contour Model with Automatic Initialisation

Deformable models represent algorithms for segmentation images by the contour. The introduction of these models in image processing was done by Kass et al. [20] who proposed the first known as "active contours" model. Then, the idea has been widely adopted and developed to give rise to several other models depending on the particular problems and the nature of the processed images. We have grouped these models into three main classes, namely (i) parametric models whose curve is explicitly represented by a parametric function, (ii) geometric models whose curve is represented implicitly considered the border of level zero of a function, and (iii) higher order statistical models that are based on a preliminary statistical analysis of the variation structures. All these models admit an interesting property, which is the integration of a priori knowledge about the structures of interest in the process of segmentation. They have proven their performance in several application areas [20]-[23].

The ASM is a variation of deformable statistical models, which is introduced by Cootes and al. [20] in order to extract complex and non-rigid objects. The advantage of the ASM compared to other variants of deformable models is that the evolution of the curve is guided by a strong a priori knowledge about the geometry and deformation modes of the structure studied. This knowledge is represented by a statistical model which describes the authorized deformation space. The construction of such a model is done by applying a Principal Component Analysis (PCA) on a training set, which includes the various possible forms of the object [24]-[26].
The shape is defined by the following equation:

$$\upsilon = \bar{\upsilon} + P_f\, b_f \qquad (1)$$

were $\bar{\upsilon}$ the average shape, P_f matrix of the main modes of the deformation’s shape and b_f a weight matrix representing the projection of the form υ in the database P_f.

The segmentation of dynamic structures in medical imaging is one of the most difficult problems that continues to preoccupy researchers. This problem arises especially in the manual initiation of the mean shape. To address this problem, we have integrated the concept of a priori knowledge to our automatic initialization to make the task of automatic segmentation and avoid manual initiation.

N feature points are positioned on the contour of the region of interest. Each form will be modeled by a vector constructed by concatenating the coordinates of points placed on the contour:

$$V_i = (X_{i1}, Y_{i1}, X_{i2}, Y_{i2}, X_{i3}, Y_{i3}, \ldots\ldots X_{in}, Y_{in}) \qquad (2)$$

where (X_{ij}, Y_{ij}) are the coordinates of point j in image i.
Our objective is to extract an average position; so, we will take a point of each vector:

$$D_i = (X_{i\,min}, Y_{i\,min}) \qquad (3)$$

where $(X_{i\,min}, Y_{i\,min})$ is a point in the vector V_i.

$$X_{i\,min} = \min(X_{ij}) \qquad (4)$$

Applying an analysis PCA, we can deduce the modes and the amplitudes of the change of position. This phase allows to

Copyright (c) IARIA, 2015. ISBN: 978-1-61208-390-2

build the model describing the position variation range of the authorized position of the structure studied.

This model is defined by the following equation:

$$D=D_m + P_d b_d \qquad (5)$$

where D_m is the average position, P_d the matrix of the variation modes of position and b_d the projection of the position D on the base P_d.

C. Extract Feature

The notion of form is very important because it allows us to identify the objects that surround us. The shape analysis is considered successful if it is used to describe objects in a manner similar to human perception of shapes. Color is used as a descriptor. We put the area of the CC segmented on a black background. After extracting the region of the CC, the surface and the standard deviation of this area will be calculated.

It is necessary to count the pixel number of a colored area.

X_{ij} is the pixel coordinates i, j.

nbl: number of rows.   nbc: number of columns.

$$Surface = \sum_{i=0}^{nbl} \sum_{j=0}^{nbc} X_{ij} \qquad (6)$$

The standard deviation is defined in probability and applied statistics. Statistically, it is a measure of spread data. It is defined as the square root of the variance, or equivalently as the quadratic mean of the deviations from the average. It has the same size as the random variable or the statistical variable.

If X is a random variable square-integrable, so belonging to the space $L^2(\Omega,A,P)$, standard deviation, usually denoted, is defined as the square root of the expected value of (X-E [X]) ²:

$$\sigma_X = \sqrt{E[(\mathrm{X} - \mathrm{E[X]})]^2} \qquad (7)$$

where E[x], the expected value of a real random variable is intuitively the value you expect to find, on average, if the same random experiment is repeated many times. It is written E[X]. If the variable X has a countable infinity of values x1, x2... with probabilities p1, p2,..., X expectancy is defined as:

$$E[\mathrm{X}] = \sum_{i=1}^{\infty} X_i p_i \qquad (8)$$

The lower the standard deviation is, the more homogeneous the study area is. Conversely, if it is more important, the area is more heterogeneous.

D. Classification

Decision trees [27] are tools for decision support. They consist of a set of rules for dividing a set of cases in homogeneous groups. Each rule involves a combination of tests on the descriptors of a case to a group. These rules are organized as a tree whose structure has the following meaning:

- Each node corresponds to the test.
- Each arc corresponds to the response test.

More generally, decision trees can handle any type of descriptor, provided a method available to group cases according to the descriptor. Since each test is applied to a single descriptor at a time, decision trees are well suited to handle heterogeneous cases.

For classification, we propose the following method: our database contains two types of images: reached and healthy. Each image is recorded by the initial vector of the contour, the surface and the standard deviation of the CC. The extraction of the region of interest is achieved by placing 30 points on the initial contour of the CC. If an image is to be tested one should determine the maximum surface for reached images and fixed as a threshold. For the standard deviation (std), we determine the least std for reaches images and fixed as a threshold deviation. For our database there were two thresholds, namely, a threshold of surface S_{surf} 3000 pixels and a threshold of standard deviation is 23 S_{dev}.

The diagram in Figure 2 shows the stages of our classification.

S_{obt}: surface obtained

Std_{obt} : standard deviation obtained

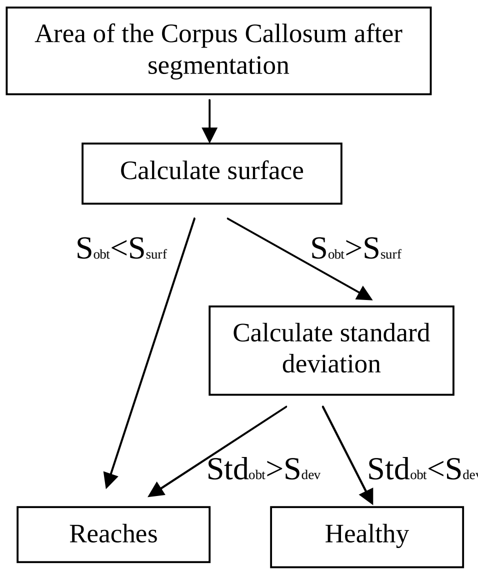

Figure.2. Diagram of the Classification algorithm

For the classification of an image after the extraction of the area of the CC, the surface of this area is determined.

- If the resulting surface is less than the threshold S_{surf} area, then the subject is directly classified as reached.
- Otherwise, the standard deviation (std) of the CC area is determined.
    - If the std exceeds the S_{dev}, then the subject is reached.
    - Otherwise, the subject is classified as normal.

 ISBN: 978-1-61208-390-2

<u>Classification Algorithm</u> :

```
// Step 3: Step of classification
// the surface of the Corpus Callosum Sobt was determined

        If (Sobt <Ssurf)
             Text ('Topic reached');
         else
// the standard deviation Stdobt  is determined

           If (Stdobt <Sdev)
              Text (normal Subject);
           else
              Text ('Topic reached');
```

Figure 3. Classification Algorithm

VI. RESULTS AND DISCUSSION

Segmentation is considered as the initial stage in the CAD, especially if one disregards the pretreatment stage which, according to the previous section, is not essential when processing masses. The segmentation phase is very important because the subsequent treatments (description and classification) are strongly related to the segmentation result. Indeed, a good detection of the contour of the lesion yields a true description of its characteristics. Thus, one can ensure a classification minimizing false positive rate and maximizing the rate of true negatives.

Our approach was tested on 50 images including 40 images have healthy subjects. We limit ourselves to show the results obtained for a healthy image and an image for the case reached.

Figures 4 and 5 show sample-result MRI localization obtained from a healthy and reached subject.

The first row shows the image and the original contour and the second line shows the results obtained with the application of the ASM model.

After the execution of the classification algorithm, we find the value 3000 pixels as the threshold surface and 23 as the threshold deviation.

Table I gives the values for the two studied subjects as well as the classification comparing the surface and standard deviation by the thresholds.

Subject 1:

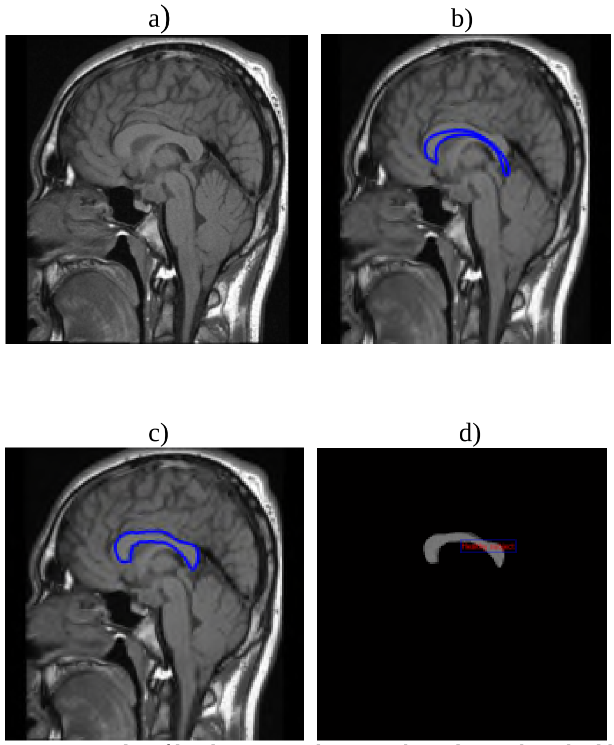

Figure 4. Examples of localization results on synthetic data: Subject healthy. (a) Original image (b) Original contour (c) Final contour (d) region detected

Subject 2:

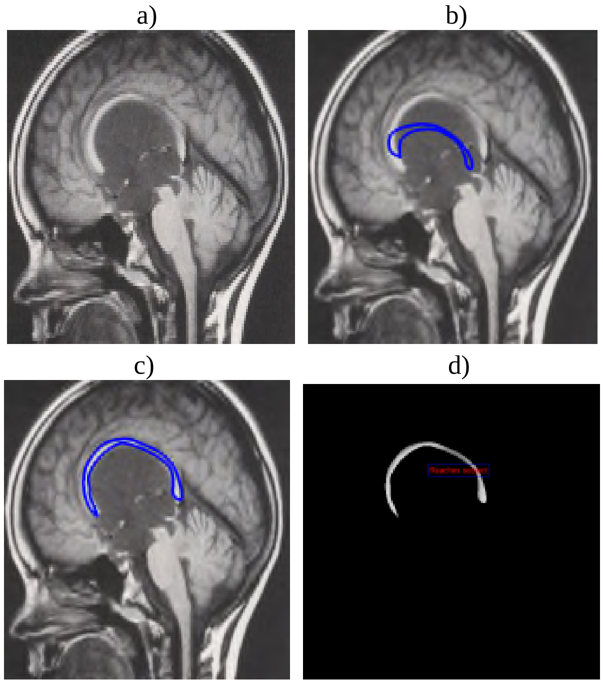

Figure 5. Examples of localization results on synthetic data: Subject reached. (a) Original image (b) Original contour (c) Final contour (d) region detected

 ISBN: 978-1-61208-390-2

TABLE I. VALUES OF THE SURFACE AND THE STANDARD DEVIATION

	Surface CC (pixel)	Standard Deviation
Subject 1 Healthy Subject	3120	13.1
Subject 2 Reaches Subject	2450	-

The surface of the CC for subject 1 is equal to 3120 pixels; this number is above the threshold surface so we move to calculate the standard deviation, which is equal to 13.1, and this is less than the standard deviation threshold therefore this subject is classified as healthy. The CC surface for subject 2 is equal to 2450 pixels is less than the threshold surface so this is classified directly as reached.

Using the calculation of standard deviation, we can analyze the region of the CC in a more robust manner. Our method can be applied on both sides of the brain. If one of the two parties does not satisfy the conditions, then we are in the case of the reached subject. The advantage of ASM is that the evolution of the curve is guided by a strong a priori knowledge about the geometry and deformation modes of the studied structure. This knowledge is represented by a statistical model which describes the authorized deformation.The construction of such model is done by applying a principal component analysis on a training set, which includes the various possible forms of the object. This model converges with the desired contours and the classification method has given us effective results. The results suggest that coprus callosum shape may be a more sensitive marker than its size for monitoring the evolution of Alzheimer disease.

We have appied the two supervised classification (k-nearest neighbors KNN [28] and decision tree [29]) methods with 50 images (40 normal and 10 AD). The KNN algorithm is among the simplest machine learning algorithms.

TABLE 2. RESULT CLASSIFICATION USING THE 2 METHODS

	TR	TFP	TFN
Decision Tree	39	5	6
KNN	35	6	9

We see that the decision tree is better than the KNN.

IV. CONCULSION AND FUTURE WORK

We proposed an approach to detect Alzheimer's diseases, based on deformable model for segmentation of the Corpus Callosum. In a first step, we used the median filter to avoid noise in the image. Then, we added a priori knowledge to the manual initialization of the mean shape to make this step automatic. After extraction of the Corpus Callosum, we used a classification method that brings in a decision tree. As perspective for this work, we propose to use a method of supervised classification as SVM (Support Vector Method).

REFERENCES

[1] Bosc, M., Heitz, F., Armspach, J.-P., Namer, I., Gounot, D. and Rumbach, L.: Automatic change detection in multimodal serial MRI: application to multiple sclerosis lesion evolution, 2003, NeuroImage 20, 643–656

[2] Radke, R.J., Andra, S., Al-Kofahi, O. and Roysam, B.: Image change detection algorithms: a systematic survey. IEEE Trans, 2005, Image Process 14(3), 294–307

[3] Bosc, M., Heitz, F., Armspach, J.-P., Namer, I., Gounot, D. and Rumbach, L.: Automatic change detection in multimodal serial MRI: application to multiple sclerosis lesion evolution. 2003, NeuroImage 20, 643–656

[4] Rey, D., Subsol, G., Delingette, H. and Ayache, N.: Automatic detection and segmentation of evolving processes in 3D medical images: Application to multiple sclerosis. In: Kuba, A., S´amal, M., Todd-Pokropek, A. (eds.) IPMI 1999. LNCS, Springer, Heidelberg 1999, vol. 1613, pp. 154–157.

[5] Ashburner J and Friston KJ. Voxel-based morphometry the methods. Neuroimage. 2000 Jun; 11(6 Pt 1):805-21.

[6] O. Ben Ahmed, J. Benois-Pineau, C Ben Amar, M. Allard and G. Catheline , Early Alzheimer disease detection with bag-of-visual-words and hybrid fusion on structural brain mri, Content-Based Multimedia Indexing'2013, Veszprêm: Hungary 2013.

[7] S. Ettaieb, K. Hamrouni and S. Ruan. Statistical modelsof shape and spatial relation-application to hippocampus segmentation. 9th International Conference on Computer Vision Theory and Applications (Visapp), Lisbon- Portugal, Janvier 2014.

[8] Cabezas M, Oliver A, Llado´ X, Freixenet J and Cuadra MB (2011) A review of atlas-based segmentation for magnetic resonance brain images. Comput Methods Programs Biomed 104:e158–e177

[9] Di Paola M, Di Iulio F, Cherubini A, Blundo C, Casini AR,Sancesario G, Passafiume D, Caltagirone C and Spalletta G (2010) When, where, and how the corpus callosum changes in MCI and AD: a multimodal MRI study. Neurology 74:1136–1142

[10] Di Paola M, Luders E, Di Iulio F, Cherubini A and Passafiume D,Thompson PM, Caltagirone C, Toga AW and Spalletta G (2010) Callosal atrophy in mild cognitive impairment and Alzheimer's disease: different effects in different stages. Neuroimage 49:141–149

[11] Di Paola M, Spalletta G and Caltagirone C (2010) In vivo structural neuroanatomy of corpus callosum in Alzheimer's disease and mild cognitive impairment using different MRI techniques: a review. J Alzheimers Dis 20:67–95

[12] Frederiksen KS, Garde E, Skimminge A, Ryberg C, Rostrup E, Baare´WF, Siebner HR, Hejl AM, Leffers AM and Waldemar G (2011) Corpus callosum atrophy in patients with mild Alzheimer's disease. Neurodegener Dis 8:476–482

[13] Hampel H, Teipel SJ, Alexander GE, Horwitz B, Teichberg D and Schapiro MB, Rapoport SI (1998) Corpus callosum atrophy is a possible indicator of region- and cell type-specific neuronal degeneration in Alzheimer disease: a magnetic resonance imaging analysis. Arch Neurol 55:193–198

[14] Hampel H, Teipel SJ, Alexander GE, Horwitz B, Teichberg D and Schapiro MB, Rapoport SI (1998) Corpus callosum atrophy is a possible indicator of region- and cell type-specific neuronal degeneration in Alzheimer disease: a magnetic resonance imaging analysis. Arch Neurol 55:193–198

[15] Teipel SJ, Bayer W, Alexander GE, Bokde AL, Zebuhr Y, Teichberg D, Mu¨ller-Spahn F, Schapiro MB, Mo¨ller HJ, Rapoport SI and Hampel H (2003) Regional pattern of hippocampus and corpus callosum atrophy in Alzheimer's disease in relation to dementia severity: evidence for early neocortical degeneration. Neurobiol Aging 24:85–94

[16] Thomann PA, Wustenberg T, Pantel J, Essig M and Schroder J (2006) Structural changes of the corpus callosum in mild cognitive impairment and Alzheimer'sdisease. Dement Geriatr Cogn Disord 21:215–220

[17] Wang PJ, Saykin AJ, Flashman LA, Wishart HA, Rabin LA, Santulli RB, McHugh TL and MacDonald JW, Mamourian AC (2006) Regionally specific atrophy of the corpus callosum in AD, MCI and cognitive complaints. Neurobiol Aging 27:1613–1617

[18] Weis S, Jellinger K and Wenger E (1991) Morphology of the corpus callosum in normal aging and Alzheimer's disease. J Neural Transm Suppl 33:35–38

[19] Zhu M, Gao W, Wang X, Shi C and Lin Z (2012) Progression of corpus callosum atrophy in early stage of Alzheimer's disease: MRI based study. Acad Radiol 19:512–517.

[20] T. Cootes, C. Taylor, D. Cooper and J. Graham. Active Shape Models – Their Training and Application. Computer Vision and Image Understanding, January 1995,vol. 61, No. 1, pp 38-59.

[21] S. Ettaieb, N. Khlifa and K. Hamrouni. Follow up of the left ventricle movement in dynamic scintigraphic images based on a spatio-temporal priori knowledge.4th International Symposium on Image/Video Communications over fixed and mobile networks. ISIVC 2008. Bilbao Spain. July 9-11, 2008

[22] H. Ghassan and T Gustavsson. Combining Snakes and Active Shape Models for Segmenting the Human Left Ventricle in Echocardiography Images. IEEE Computers in Cardiology, 2000, Vol 27.

[23] P. He and J. Zheng. 'Segmentation of tibia bone in Ultrasound images using Active Shape Models'.23rd Annual Conference– IEEE/EMBS, Istanbul,TURKEY. Oct 2001

[24] T. Cootes, A. Hill, C. Taylor, and J. Haslam. The use of active shape models for locating structures in medical images. Image and Vision Computing 12(6):355- 366. 1994

[25] Z. zheng and F. yang . Enhanced active shape model for facial feature localization Proceedings of the Seventh International Conference on Machine Learning and Kunming, 12-15 July 2008.

[26] Matthias Seise, Stephen J. McKenna and Carlos A. Wigderowitz. Learning Active Shape Models for Bifurcating Contours. IEEE transactions on medical imaging, may 2007, vol. 26, no. 5.

[27] L. Breiman, J. Friedman, R. Olshen and C. Stone, Classification and regression trees, Wadsworth & Brooks, 1984.

[28] Hechenbichler, K. and Schliep K. (2004) Weighted k-nearest-neighbor techniques and ordinal classification. Sonderforschungsbereich 386, paper 399.

[29] L. Breiman, J. Friedman, R. Olshen and C. Stone, Classification and regression trees, Wadsworth & Brooks, 1984.